Measurements of Charge Symmetry Violating Quark Distributions

J. Arrington, A. El Alaoui, L. El Fassi, D. F. Geesaman, K. Hafidi(Co-Spokesperson), R. J. Holt, H. E. Jackson, D. Potterveld, B. Mustapha(Co-Spokesperson), P. E. Reimer, E. C. Schulte, X. Zheng

Argonne National Laboratory

C. Keppel, M. Christy

Hampton University

A. Ahmidouch, S. Danagoulian

North Carolina A&T State University

P. Bosted, V. Dharmawardane, R. Ent, D. Gaskell, M. Jones

Thomas Jefferson National Accelerator Facility

E. J. Beise, J. J. Kelly

University of Maryland

R. Asaturyan, H. Mkrtchyan, T. Navasardyan, V. Tadevosyan

Yerevan Physics Institute, Yerevan, Armenia

December 6^{th}, 2004

Abstract

We propose to measure semi-inclusive charged pion electroproduction on deuterium in the deep inelastic scattering region. These measurements use 6 GeV electron beam and will be performed for two x bins centered respectively around 0.35 and 0.45 for four z bins corresponding to 0.5, 0.55, 0.6 and 0.65. The goal of this experiment is to extract the charge symmetry violating contributions in the valence quark distribution functions. No direct measurements exist to date; however they are possible now because of the high luminosity available at Jefferson Lab. These data are of great importance and can shed light on various exciting subjects such as the NuTeV anomaly. Several theoretical works suggested that valence quark charge symmetry violation is the most likely candidate to cure this anomaly.

1 Introduction

Everybody agrees on the importance of testing fundamental symmetries, even approximate ones. In this proposal we are interested in measuring charge symmetry violation in valence quark distributions. In parton distribution functions, it is routinely assumed that charge symmetry is valid. Surprisingly enough, there are no direct measurements of such a contribution, and this makes these measurements even more important. Measurement of a nonzero effect would be extremely interesting and will have various important implications on recent topics such as the measurement of Weinberg angle using neutrino deep inelastic scattering. Semi-inclusive deep inelastic scattering on deuterium can be used to probe charge symmetry violation effects. Charged pions will be detected in coincidence with the scattered electrons. Efficient detection of both signs of charged pions is important, but absolute yields are not required as overall normalizations cancel out in the measured ratio.

The organization of this proposal is as follows. In section 2, we discuss the physics motivation and the important implications of these measurements. Section 3 discusses the validity of factorization assumption for JLab energies. In section 4, we review the formalism for semi-inclusive pion production on deuterium. The experimental details and rates are given in section 5. Section 6 gives the beam time request. Different corrections and corresponding systematical errors are discussed in section 7. Finally, expected precision is presented in section 8.

2 Physics Motivation

Symmetries are the key to understanding and classifying the structure of matter and the fundamental forces and their study leads to better understanding of the underlying physics. With the advances in experimental and theoretical tools, symmetries other than those of space-time were introduced in physics. Isospin (IS) and charge (CS) symmetries are examples. They are not exact symmetries in nuclear systems. While IS requires invariance under all rotations in isospin space such that the Hamiltonian of the system commutes with the isospin operator (T), *i.e.*

$$[H, T] = [H, T^2] = 0,$$

CS is related to only one rotation. It requires invariance with respect to rotations of 180^o about the T_2 axis, where the charge corresponds to the third axis. If CS is a valid symmetry the Hamiltonian has to commute with the charge symmetry operator P_{CS}, *i.e.*

$$[\mathrm{H},\ \mathrm{P}_{CS}] = 0, \ \text{ where } \ \mathrm{P}_{CS} = \exp(\mathrm{i}\pi T_2),$$

Consequently, IS implies CS but not the converse. CS is used to understand many relations between strong interaction processes. For details we refer the reader to comprehensive reviews by Miller, Nefkens and Slaus [1], and Henley and Miller [2]. For nuclei, the CS operator interchanges neutrons and protons. Thus, CS implies the equality of the neutron-neutron and proton-proton interaction. Also, it requires that two mirror reactions in isospin space have the same cross section, e.g., $\sigma(\mathrm{n},{}^3\mathrm{He}) = \sigma(\mathrm{p},{}^3\mathrm{H})$. Furthermore, CS predicts the equality of mirror nuclear masses, e.g., $\mathrm{m}({}^3\mathrm{He}) = \mathrm{m}({}^3\mathrm{H})$, and it establishes relationships between spin and polarization observables.

At the quark level, P_{CS} acts only on the two light quark flavors:

$$\mathrm{P}_{CS}|\mathrm{d}\rangle = |\mathrm{u}\rangle \ \text{ and } \ \mathrm{P}_{CS}|\mathrm{u}\rangle = \text{-}\ |\mathrm{d}\rangle,$$

CS implies the invariance of a system under the interchange of up and down quarks while simultaneously interchanging protons and neutrons, *i.e.*

$$u^p(x, Q^2) = d^n(x, Q^2)$$

$$d^p(x, Q^2) = u^n(x, Q^2)$$

Quantum Chromo-Dynamics (QCD) provides a clear formulation of the origin of charge symmetry violation (CSV). In QCD, the only sources of CSV are electromagnetic interactions and the mass difference $\delta m = m_d - m_u$ between down and up quarks. Electromagnetic interactions should play a minor role at high energies. Thus, the light quark mass difference is the interesting feature of the QCD view of CSV [3].

CS is a more restricted symmetry than IS; therefore it is generally conserved in strong interactions to a greater degree than IS. Isospin violating forces produce large differences betwen nn and np scattering lengths and effective ranges in the ${}^1\mathrm{S}_0$ state. The effect of isospin violating forces is large at low energies because the ${}^1\mathrm{S}_0$ state is almost bound. Charge symmetry appears to be more respected than isospin symmetry [2]. The difference between nn and pp (after correction for direct electromagnetic effects) scattering lengths is small or zero; the difference in the corresponding effective ranges is hard to determine. Thus, while in many nuclear reactions IS is violated at the few percent level, in most cases CS is obeyed to better than one percent: the proton and neutron masses are equal to about 1%; the binding energies of tritium and ^{3}He are equal to 1%, after Coulomb corrections. By comparing energy levels in mirror nuclei, one generally finds agreement to better than 1%, after correcting for electromagnetic interactions. At the parton level, one would naively expect CSV to be of the order of the up-down current quark mass difference divided by some average mass expectation value of the strong Hamiltonian, *i.e.*, $(m_d - m_u)/ < M >$, where <M> has a value roughly 0.5-1.0 GeV. This would put CSV effects at a level of 1% or smaller [4].

From our experience with CS in nuclear systems, and because of the order of magnitudes estimates of CSV in parton systems, CS has been universally assumed in quark distribution functions. It is so common in quark-parton phenomenology that it is frequently not even mentioned as an assumption. CS reduces by a factor of two the number of independent quark distributions necessary to describe high energy data, and until recently there has been no compelling reason to suggest CSV. On the other hand, there were no precise tests of charge symmetry in parton distributions. Recently much attention has been focused on the apparent violation of what is called SU(2) flavor symmetry in the nucleon. This was suggested by New Muon Collaboration (NMC) [5] and later supported by results from NA51 group at CERN [6] and E866 Drell-Yan experiment [7] at FNAL. Experimental results from these collaborations seem to show a large flavor symmetry violation in the proton sea quark distributions (i.e. $\bar{u}^p(x) \neq \bar{d}^p(x)$). However this could also in principle be explained even if flavor symmetry were conserved, if we assume CSV in the nucleon sea. The valence quark CSV is also a very important issue because it makes a substantially larger contribution than the sea quark CSV to the extraction of the Weinberg angle from neutrino Deep Inelastic Scattering (DIS). The three standard deviation result from the Standard Model prediction reported by NuTeV collaboration [8] or the so called "NuTeV anomaly" could be completely removed by assuming valence quark CSV.

In this proposal, we are interested in CSV in valence quark distributions. At present, there are no direct measurements that reveal the presence of CSV in parton distribution functions. We have only upper limits on the magnitude of CSV. These limits arise from comparing the structure function F_2^ν measured in neutrino induced charged current reactions, and the structure function F_2^γ for charged lepton DIS, both measurements on isoscalar targets [9]. The most precise neutrino measurements were obtained by the CCFR collaboration [13], who extracted the F_2^ν structure function for neutrino and anti-neutrino interactions on iron at FNAL. The NMC collaboration performed the most precise measurements of F_2^γ structure functions using muon interaction on deuterium at $\mathrm{E}_\mu = 90$ and 280 GeV. In the region of $0.1 \leq x \leq 0.4$, an upper limit of 9% was set for CSV effects.

Several theoretical investigations of CSV in valence quark distributions have been carried out initially by Sather [14] and by Rodionov et al [15]. They calculated valence quark distributions for the proton and neutron in a quark model and in the MIT bag model, respectively. In both models, $u^p(x)$ and $d^n(x)$ satisfied CS to within 1% while $d^p(x)$ and $u^n(x)$ were predicted to violate charge symmetry by 5% or more at large x values. In addition, both calculations predict opposite signs for $\delta u_v = u_v^p(x) - d_v^n(x)$ and $\delta d_v = d_v^p(x) - u_v^n(x)$ in the valence region.

Because theoretical estimates put parton CSV at the percent level and because of the lack of direct evidence for violation of parton charge symmetry, all previous phenomenological parton distribution functions have assumed the validity of parton charge symmetry. However, MRST group [16] have recently studied the uncertainties in parton distribution functions (PDFs) arising from a number of factors, including charge symmetry violation. They constructed a functional form for CSV component that automatically satisfied the quark normalization condition:

$$\int_0^1 dx \delta d_v(x) = \int_0^1 dx \delta u_v(x) = 0$$

where $\delta u_v(x) = -\delta d_v(x) = \kappa f(x)$. This function has the following form:

$$f(x) = (1-x)^4 x^{-0.5}(x - 0.0909)$$

The function $f(x)$ was chosen so that at both small and large x, $f(x)$ has the same form as the MRST valence quark distributions and the first moment of $f(x)$ is zero. The functional form of the valence CSV distributions guaranteed that δu_v and δd_v would have opposite signs at large x, in agreement with the theoretical calculations mentioned previously. The overall coefficient κ was then varied in a global fit to a wide range of high energy data. The value of κ which minimized χ^2 was $\kappa = -0.2$. The MRST distribution of χ^2 vs. κ has a shallow minimum with 90% confidence level obtained for the range $-0.8 \leq \kappa \leq +0.65$. In conclusion, CSV effects that are in reasonably good agreement with high energy data are substantially larger than predicted by theory; valence CSV effects could be four times as large as predicted by Sather and Rodionov or three times as large with opposite sign. For NuTeV measurements, the value $\kappa = -0.6$ would completely remove the anomaly, while the value $\kappa = +0.6$ would double the discrepancy. Note that these two values are within the 90% confidence level limit found by MRST. A recent work by J. T Londergan and A. W. Thomas [9] taking into account the MRST phenomenological analysis showed that the CSV effects are one viable explanation of the anomalous value of the Weinberg angle obtained in the NuTeV experiment. They strongly encouraged experimental investigations to directly measure CSV which can be surprisingly as large as the values obtained by MRST phenomenological fit.

3 Factorization at JLab energies

As all semi-inclusive analyses, the formalism used to extract charge symmetry violating quark distributions involves the assumption of factorization. This assumption implies that the scattering and production mechanisms factorize. To demonstrate factorization, HERMES used the flavor asymmetry ratio $(\bar{d}-\bar{u})/(u-d)$ for five x bins as a function of z. No strong indication of z dependence was observed [10]. Recently, more precise HERMES data showed no z dependence of d_v/u_v over a large range for $0.02 < x < 0.6$ to an accuracy better than 5% [11]. More evidence comes from recent measurements by E00-108 experiment [18] in Hall C. Preliminary results showed that the data are consistent with factorization for JLab energies in optimized kinematics. Figure 1 shows the semi-inclusive π^- production cross section in excellent agreement with a Monte Carlo simulation using CTEQ5 NLO parton distribution functions and the fragmentation function parameterization from Binnewies *et al.* [12]. Exception can be made for $z > 0.7$ where the discrepancy is believed to reflect the ^{1}H(e,e'π^-)Δ region.

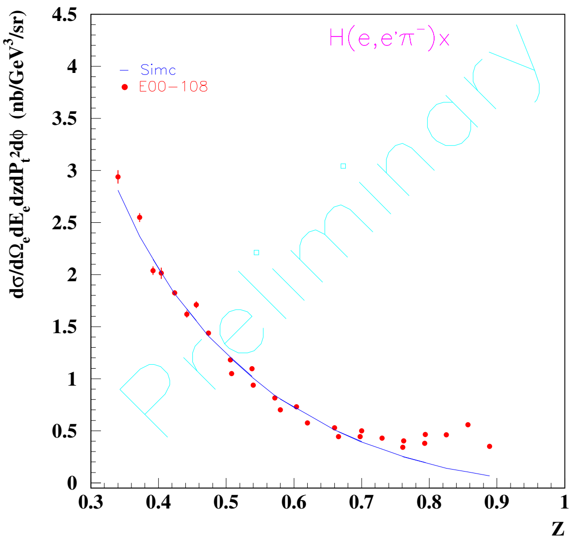

Figure 1: The ^{1}H(e,e'π^-)X cross section at x=0.32 as a function of z (solid circles) in comparison with a Monte Carlo simulation (solid curve) starting from a fragmentation ansatz (see text). The scatter of the data is due to having performed only a rudimentary bin centering.

4 Formalism

Semi-inclusive pion production from lepton deep inelastic scattering on nuclear targets was suggested [4, 17] as a sensitive probe of CSV effects in nucleon valence distributions. The authors proposed measuring the quantity $R^D_{meas}(x, z)$ defined by:

$$R^D_{meas}(x,z) = \frac{4N^{D\pi^-}(x,z) - N^{D\pi^+}(x,z)}{N^{D\pi^+}(x,z) - N^{D\pi^-}(x,z)}, \tag{1}$$

where $N^{D\pi^+}$ ($N^{D\pi^-}$) is the yield of π^+ (π^-) produced in coincidence with the scattered electron from deuterium.

In the quark-parton formalism, the semi-inclusive production of hadrons in DIS from a nucleon is given by:

$$\frac{1}{\sigma_N(x)}\frac{d\sigma^h_N(x,z)}{dz} = \frac{\sum_i e_i^2 q_i^N(x) D_i^h(z)}{\sum_i e_i^2 q_i^N(x)} \tag{2}$$

$q_i^N(x)$ is the distribution function for quarks of flavor i, and charge e_i, in the hadron N as a function of Bjorken x. $D_i^h(z)$ is the fragmentation function for a quark of flavor i into hadron h. The fragmentation function depends on the quark longitudinal momentum fraction $z = E_h/\nu$, where E_h is the energy of the hadron and ν is the energy of the virtual photon. The yield of hadron h per scattering from nucleon N can be written as $N^{Nh} = \sum_i e_i^2 q_i^N(x) D_i^h(z)$. In terms of these quantities, semi-inclusive production of a charged pion from a proton (neutron) can be described by

$$\begin{aligned} N^{p\pm}(x,z) &= \frac{4}{9}u^p(x)D_u^\pm(z) + \frac{4}{9}\bar{u}^p(x)D_{\bar{u}}^\pm(z) \\ &+ \frac{1}{9}d^p(x)D_d^\pm(z) + \frac{1}{9}\bar{d}^p(x)D_{\bar{d}}^\pm(z) \\ &+ \frac{1}{9}s^p(x)D_s^\pm(z) + \frac{1}{9}\bar{s}^p(x)D_{\bar{s}}^\pm(z), \end{aligned} \tag{3}$$

$$\begin{aligned} N^{n\pm}(x,z) &= \frac{4}{9}u^n(x)D_u^\pm(z) + \frac{4}{9}\bar{u}^n(x)D_{\bar{u}}^\pm(z) \\ &+ \frac{1}{9}d^n(x)D_d^\pm(z) + \frac{1}{9}\bar{d}^n(x)D_{\bar{d}}^\pm(z) \\ &+ \frac{1}{9}s^n(x)D_s^\pm(z) + \frac{1}{9}\bar{s}^n(x)D_{\bar{s}}^\pm(z) \end{aligned} \tag{4}$$

Charge Conjugation invariance implies that $D_u^\pm = D_{\bar{u}}^\mp$ and $D_d^\pm = D_{\bar{d}}^\mp$. By making the additional assumption of charge symmetry, the fragmentation functions will obey the relations:

$$\begin{aligned} D_d^{\pi^-}(z) &= D_u^{\pi^+}(z) \\ D_d^{\pi^+}(z) &= D_u^{\pi^-}(z), \end{aligned} \tag{5}$$

and the parton distribution functions will satistfy the relations:

$$\begin{aligned} u^p(x) &= d^n(x) \\ d^p(x) &= u^n(x) \end{aligned} \tag{6}$$

Using Eqs (3), (4), (5) and (6), one can derive the expression for R^D_{meas}

$$\begin{aligned} R^D_{meas}(x,z) &= \frac{5\Delta(z)}{1-\Delta(z)} + 5\left[\frac{1+\Delta(z)}{1-\Delta(z)}\right] \times \frac{[\bar{u}^p(x)+\bar{d}^p(x)]}{[u^p_v(x)+d^p_v(x)]} \\ &+ \left[\frac{\Delta_s(z)}{1-\Delta(z)}\right]\frac{[s(x)+\bar{s}(x)]}{[u^p_v(x)+d^p_v(x)]}, \end{aligned} \tag{7}$$

where

$$\Delta(z) = \frac{D_u^{\pi^-}(z)}{D_u^{\pi^+}(z)}, \tag{8}$$

and the strange-favored ratio of the quark fragmentation functions

$$\Delta_s(z) = \frac{D_s^{\pi^+}(z) + D_s^{\pi^-}(z)}{D_u^{\pi^+}(z)} \tag{9}$$

In Eq. (7), we assume the validity of the impulse approximation, *i.e.*,

$$N^{D\pi^\pm}(x,z) = N^{p\pi^\pm}(x,z) + N^{n\pi^\pm}(x,z) \tag{10}$$

In Eq. (7), charge symmetry was also assumed in PDFs and fragmentation functions. Keeping charge-symmetry-violating functions, the $R^D_{meas}(x,z)$ ratio becomes:

$$\begin{aligned} R^D_{meas}(x,z) &= \frac{5\Delta(z)}{1-\Delta(z)} - \frac{[4+\Delta(z)]\delta D(z)}{3[1-\Delta(z)]^2} \\ &+ \left[\frac{1+\Delta(z)}{1-\Delta(z)}\right] \times \left[\frac{4[\delta d(x)-\delta u(x)] + 15[\bar{u}^p(x)+\bar{d}^p(x)]}{3[u^p_v(x)+d^p_v(x)]}\right] \\ &+ \left[\frac{\Delta_s(z)}{1-\Delta(z)}\right]\frac{[s(x)+\bar{s}(x)]}{[u^p_v(x)+d^p_v(x)]} \end{aligned} \tag{11}$$

The quantity R^D_{meas} in Eq. (11) contains the charge-symmetry-violating quark distribution functions

$$\begin{aligned} \delta d(x) = d^p(x) - u^n(x) \\ \delta u(x) = u^p(x) - d^n(x), \end{aligned} \tag{12}$$

and the charge symmetry-breaking fragmentation functions

$$\delta D(z) = \frac{D_u^{\pi^+}(z) - D_d^{\pi^-}(z)}{D_u^{\pi^+}(z)} \tag{13}$$

A more clean separation of the x and z dependence can be obtained by multiplying R^D_{meas} by a z-dependent factor, e.g.

$$\tilde{R}^D(x,z) = R^D_f(z) + R^D_{CSV}(x) + R^D_{sea}(x,z) \tag{14}$$

where

$$\begin{aligned}
\tilde{R}^D(x,z) &= \frac{1-\Delta(z)}{1+\Delta(z)} R^D_{meas}(x,z), \\
R^D_f(z) &= \frac{5\Delta(z)}{1+\Delta(z)} - \frac{[4+\Delta(z)]\delta D(z)}{3[1-\Delta^2(z)]}, \\
R^D_{CSV}(x) &= \frac{4[\delta d(x) - \delta u(x)]}{3[u_v^p(x) + d_v^p(x)]}, \\
R^D_{sea}(x,z) &= \frac{5[\bar{u}^p(x) + \bar{d}^p(x)] + \Delta_s(z)[s(x)+\bar{s}(x)]/[1+\Delta(z)]}{[u_v^p(x) + d_v^p(x)]}
\end{aligned} \tag{15}$$

Equation (11) was obtained by expanding to first order the small quantities which are $\delta d(x)$, $\delta u(x)$, $\delta D(z)$ and the sea quark distribution. Therefore we need to be in the high x region where the ratio of sea to valence quark distributions is small. The quantity $\tilde{R}^D(x,z)$ separates into three pieces. The first piece $R^D_f(z)$ depends only on z. It contains a small part which is proportional to the CSV part of the fragmentation function. The dominant piece of $R^D_f(z)$ has the form $5\Delta(z)/(1+\Delta(z))$. The second term $R^D_{CSV}(x)$ depends only on x, and is proportional to the nucleon CSV term. $R^D_{sea}(x,z)$ is proportional to the sea quark distributions and can be written as a sum of a strange sea term $R^D_{sea\_S}$ and a non strange sea term $R^D_{sea\_NS}$, where

$$R^D_{sea\_S}(x,z) = \frac{\Delta_s(z)[s(x)+\bar{s}(x)]/[1+\Delta(z)]}{[u_v^p(x) + d_v^p(x)]} \tag{16}$$

$$R^D_{sea\_NS}(x) = \frac{5[\bar{u}^p(x) + \bar{d}^p(x)]}{[u_v^p(x) + d_v^p(x)]} \tag{17}$$

Experimentally, one needs to measure accurately the x dependence of $\tilde{R}^D(x,z)$ for fixed z values. The sea quark distribution should fall off monotonically and rapidly with x. So, if one goes to sufficiently large x, the sea quark contribution will be negligible relative to the CSV term. The CSV contribution of the fragmentation function to the z-dependent term $R^D_f(z)$ was estimated [17] to be 1%. Therefore it can be neglected in the expression of $R^D_f(z)$ which becomes

$$R_f^D(z) \cong \frac{5\Delta(z)}{1+\Delta(z)} \tag{18}$$

By rearranging eq. (14), one obtains the following equation:

$$D(z)\ R(x,z) + CSV(x) = B(x,z) \tag{19}$$

where

$$\begin{aligned}
D(z) &= \frac{1-\Delta(z)}{1+\Delta(z)}, \\
R(x,z) &= \frac{5}{2} + R^D_{meas}, \\
CSV(x) &= \frac{-4(\delta d - \delta u)}{3(u_v + d_v)}, \\
B(x,z) &= \frac{5}{2} + R^D_{sea_S}(x,z) + R^D_{sea_NS}(x)
\end{aligned} \tag{20}$$

In the proposed measurements, we would like to measure $R^D_{meas}(x,z)$ (see Eq. (1)) and thus $R(x,z)$ for seven bins in x and z. We will end up with seven equations similar to Eq. (13) and six unknowns, which are CSV(x_1), CSV(x_2), D(z_1), D(z_2), D(z_3) and D(z_4). $B(x,z)$ will be obtained from phenomenological PDFs. The chosen x values for the measurements will be in the region where $R^D_{sea\_S}$ becomes small.
For a better idea about different contributions, we will use phenomenological PDFs from CTEQ and MRST to evaluate the $B(x,z)$ term, fragmentation functions from a parameterization by Kretzer [19] and the MRST parameterization for CSV term. Figure 2 shows the contributions of different sea terms using the MRST2004 NLO parameterization. The non strange sea term of Eq. (17) is large compared to the strange term. By choosing an x value above 0.35, the strange contribution becomes negligible. The $R^D_{sea\_NS}$ term can be obtained from the parton distribution function. The uncertainties on this non strange sea term represent the main theoretical systematical uncertainties on the extracted CSV term.
Figure 3 shows the non strange sea term given by two parton distribution functions, MRST 2004 NLO and CTEQ6 NLO. The difference between the two curves is not large and is within the uncertainties given by each parameterization. Figure 4 shows the strange sea term for different z values. Note that the scale is small compared to the previous figures. The $R^D_{sea\_S}$ term is reduced when the z value increases. Therefore the measurements are somewhat favored at high z. Figure 5 shows the contributions of all x dependent terms. The previously mentioned sea contributions and the CSV contribution given by MRST phenomenological fit of high energy data. The curve corresponding to $\kappa = -0.8$ is considered as the upper limit by MRST fit and the one with $\kappa = +0.65$ is the lower

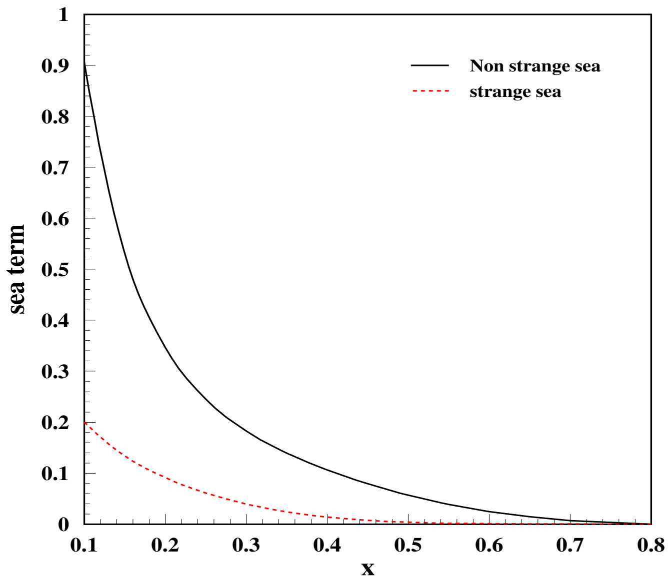

Figure 2: Solid curve corresponds to non strange sea term $R^D_{sea\_NS}(x)$. The dotted curve is the strange sea term $R^D_{sea\_S}(x,z)$.

limit. The CSV term begins to become dominant at x around 0.35. Both x of 0.35 and 0.45 were chosen for our measurements.

5 Experiment

In this experiment we propose to measure the ratio of the π^- to π^+ production yields on deuterium for different x and z bins:

$$R_Y(x,z) = \frac{Y^{\pi-}(x,z)}{Y^{\pi+}(x,z)}$$

x is the Bjorken variable and z is the fraction of the exchanged virtual photon energy carried by the pion. The reaction is shown in Fig 6.
The scattered electron and the pion will be detected in coincidence. We define E as the incident electron energy and E' and θ_e the energy and angle of the scattered electron. P_π, E_π and θ_π are the momentum, energy and angle of the detected pion, all in the Lab frame. W' is the mass of the final state without the detected pion playing the role of W in the semi-inclusive case. It is given by:

$$W'^2 = W^2 + {M_\pi}^2 - 2\ (\nu + M)\ E_\pi + |\vec{q}|\ |\vec{P_\pi}|\ cos\ \theta(\gamma^*, \pi)$$

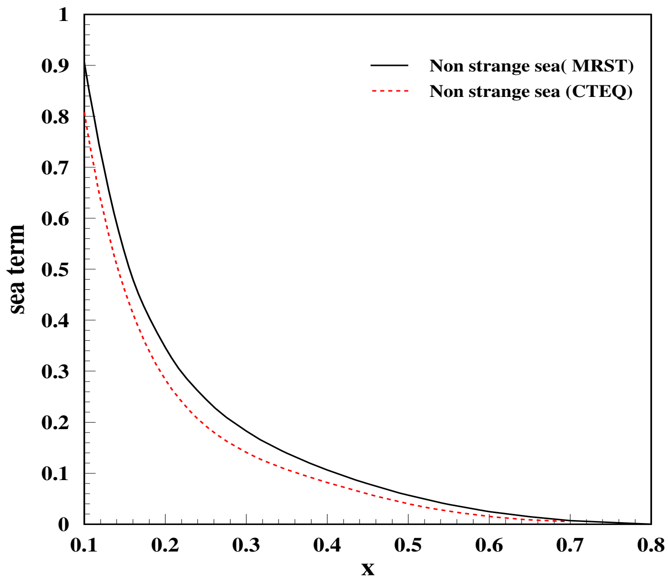

Figure 3: Solid curve corresponds to the non strange sea contribution using MRST PDF. The dotted curve is the same term using CTEQ-6M PDF.

where M and M_π are the nucleon and pion mass, respectively. $\nu = E - E'$ and $\vec{q}$ are the energy and momentum of the exchanged virtual photon. $\theta(\gamma^*, \pi)$ is the angle between the virtual photon and the pion. If we consider only pions collinear with the virtual photon and neglect the pion mass, the expression of W' simplifies to:

$$W'^2 = W^2 - 2\,(\nu + M - |\vec{q}|)\; E_\pi$$

W has the usual expression $W^2 = -Q^2 + 2M\nu + M^2$ where Q^2 is the square of the four momentum transfer given by $Q^2 = 4EE'sin^2(\theta_e/2)$.

We propose to use a 6 GeV electron beam on a liquid deuterium target and the standard Hall C equipments. The SOS will be used to detect the scattered electrons and the HMS to detect the produced pions. The installation of a small profile beam pipe downstream of the target will be needed to allow HMS to operate at angles below 12.5 degrees.

The experiment needs to cleanly identify electrons and pions. The SOS will be used as the electron arm. The combination of the lead glass shower counter and the gas Cerenkov provides pion rejection at $10^4 : 1$ for momenta above 1.5 GeV/c. The HMS will be used as the hadron arm. It will operate at both polarities. The gas Cerenkov and the lead glass calorimeter will be used for π/e separation. The time of flight is very effective in separating

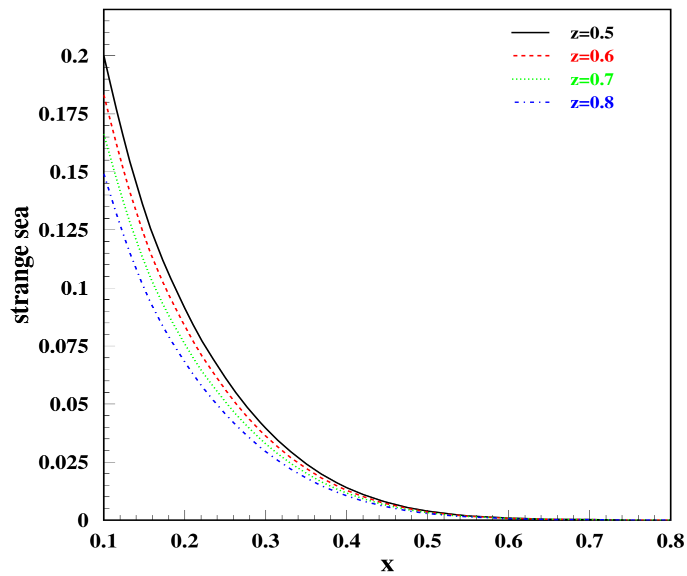

Figure 4: Strange sea term $R^D_{sea\_S}(x, z)$ for different z values as a function of x Bjorken.

π/K/p for particle momentum below 3 GeV which is our highest pion momentum. The addition of the aerogel detector recently developed and commissioned by the E00-108 collaboration enhances the capabilities of the spectrometer in distinguishing protons from pions on the level of 2.8-1.1 10^{-3} (for aerogel with n=1.03). The pion detection efficiency is better than 99% in the 1-4 GeV/c momentum range.

5.1 Kinematics

In addition to the event rates two major limits played an important role in the choice of the kinematics. The first limit is the pion momentum which needs to be larger than 2 GeV to avoid complications from πN final state interactions. Above this limit, the difference in the absorption of π^+ and π^- would not exceed the 1% [18]. The second limit is on W' which is the mass of the final state without the detected pion replacing W in the semi-inclusive case. As shown in the recent results by the E00-108 collaboration the ratio of the π^+ to π^- yields becomes flat for $W' > 1.6$ GeV suggesting the validity of the factorization hypothesis. The choice of the x and z bins should then respect these limits. Another important consideration is to point the hadron arm (HMS) into the direction of the exchanged virtual photon to ensure a symmetric coverage in the azimuthal angle of pions coming from fragmentation. Table 1 presents the central kinematics proposed for this experiment.

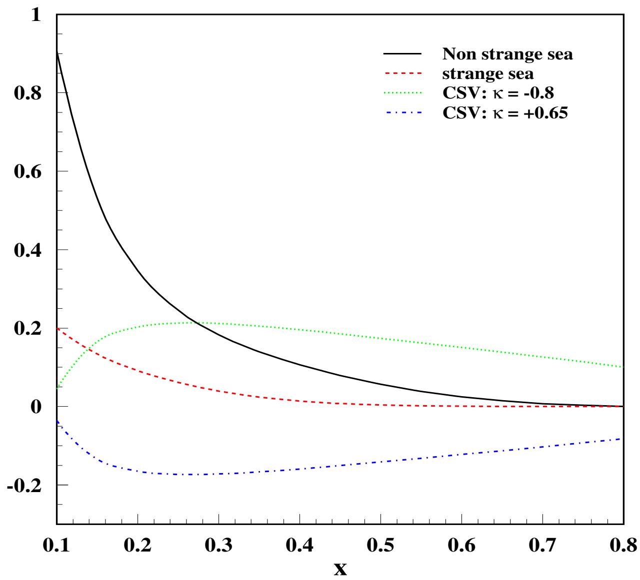

Figure 5: Contibutions of all x-dependent terms: solid curve is the non strange sea term, the dashed curve is the strange sea term, the dotted curve is the CSV term with $\kappa = -0.8$ and the dotted-dashed curve is the CSV contribution for $\kappa = +0.6$

The high scattered electron energy is dictated by both the event rates and the lowest HMS angle of 10.5 degrees (after installing the additional beam pipe). Two x bins are considered x=0.35 and 0.45. For x=0.35 the maximum z value keeping $W' > 1.6$ GeV to avoid the resonance structures is 0.66 . For x=0.45, the highest z possible decreases to 0.6. The lower limit in z is 0.5 to ensure that the pion is produced by the fragmentation process. The x=0.55 bin was excluded from these measurements because of the significantly low rate which would require double or even triple the beam time. The only allowed z with $W' > 1.6$ GeV in this case is 0.5. Four z values (z=0.5, 0.55, 0.60 and 0.65) will be measured for x=0.35 and three z values (z=0.5, 0.55, 0.60) for x=0.45.

5.2 Count rate estimate

To estimate coincident $(e, e'\pi^{\pm})$ event rates, we used the code PYTHIA (version 6.222) with the CTEQ-5M parameterization of the parton distribution functions (PDF) to generate DIS events with $Q^2 > 1$ and $W > 2$. The cross section of the generated sample was checked against the code LEPTO (version 6.5.1) and found to agree well. The Monte-Carlo simulation code SIMC was used to find the optimum spectrometer settings for these measurements and determine realistic coincident $(e, e'\pi^{\pm})$ event rates from the sample of

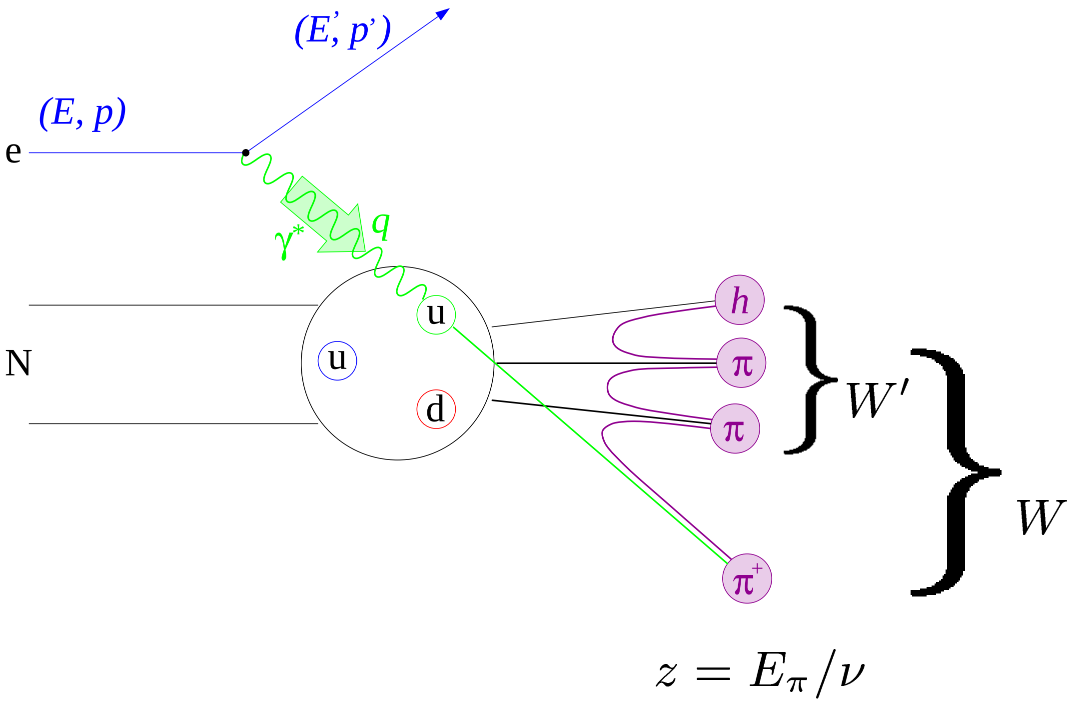

Figure 6: Semi-inclusive deep inelastic scattering process

generated events.

Since the HMS will be used at forward angles (10.5-12.5 degrees), the maximum luminosity will be limited by the rate of particles reaching its first hodoscope plane which should remain below 600-700 kHz. For this reason, we propose to use a 50 μA beam current on a 4 cm deuterium target. In this case, the highest particle rates, corresponding to the most forward angle (10.96 degree) and the lowest hadron momentum (2.13 GeV/c), are about 500 kHz for the positive polarity and 600 kHz for the negative polarity. Table 2 gives the coincident (e,e'π) event rates and the required beam time for each spectrometer setting and for both π^+ and π^-. Based on recent experimental data from E00-108 experiment [18] which were taken at similar conditions [20], the accidental-to-true coincidence ratio was found to be 1:4 in the worst case.

The beam time is estimated to have ~ 2 % final statistical error (after combining the different z bins for a given x bin) on the ratio R^D_{meas}:

$$R^D_{meas} = \frac{4N^{\pi^-} - N^{\pi^+}}{N^{\pi^+} - N^{\pi^-}} = \frac{4Y^{\pi^-} - Y^{\pi^+}}{Y^{\pi^+} - Y^{\pi^-}} = \frac{4R_Y - 1}{1 - R_Y}$$

E' GeV	θ_e deg	ν GeV	Q^2 GeV^2	x	W GeV	θ_{γ^*} deg	θ_h deg	z	P_h GeV/c	W' GeV
1.74	30.0	4.26	2.80	0.35	2.46	10.96	10.96	0.50	2.13	1.84
								0.55	2.34	1.77
								0.60	2.56	1.70
								0.65	2.77	1.62
1.74	34.1	4.26	3.60	0.45	2.30	12.09	12.09	0.50	2.13	1.72
								0.55	2.34	1.66
								0.60	2.56	1.59
1.74	37.9	4.26	4.40	0.55	2.12	13.00	13.00	0.50	2.13	1.59

Table 1: Proposed (e,e'$\pi^{\pm}$) kinematics on deuterium. The last setting corresponds to x=0.55 and is excluded from these measurements (see text or table 2 for details)

E' GeV	θ_e deg	θ_h deg	P_h GeV/c	π^+ coinc rate Hz	π^- coinc rate Hz	π^+ time hours	π^- time hours
1.74	30.0	10.96	2.13	0.96	0.62	12	18
			2.34	0.89	0.56	12	18
			2.56	0.82	0.50	12	18
			2.77	0.76	0.45	12	18
1.74	34.1	12.09	2.13	0.27	0.21	66	88
			2.34	0.24	0.19	66	88
			2.56	0.25	0.18	66	88
1.74	37.9	13.00	2.13	0.071	0.057	384	480

Table 2: Count rates and beam time for each spectrometer setting and both π^+ and π^-. This calculation assumes a 50 μA electron beam on a 4 cm long deuterium target. The last setting corresponds to x=0.55 and is excluded from these measurements, it is only added to illustrate the beam time limitation of this kind of measurement.

x	0.35	0.45
$\Delta(Y)/Y\ (\pi^{\pm})$	0.77 %	0.55 %
$\Delta(R_Y)/R_Y$	1.1 %	0.78 %
$\Delta(R^D_{meas})/R^D_{meas}$ (*1 z bin*)	4.0 %	3.5 %
Nb. of z bins	4	3
$\Delta(R^D_{meas})/R^D_{meas}$ (*all z bins*)	~ 2 %	~ 2 %

Table 3: Statistical errors as function of x based on the estimated beam time.

where R_Y is the ratio of π^- to π^+ production yields defined above. The corresponding error is expressed as follow:

$$\frac{\Delta(R^D_{meas})}{R^D_{meas}} = \frac{3\ R_Y}{(4R_Y - 1)(1 - R_Y)} \frac{\Delta(R_Y)}{R_Y}$$

Both the value and the error on R_Y are needed to determine the error on R^D_{meas}. For x=0.35 PYTHIA gives a ratio R_Y of about 0.65 which is practically independent of z. This value is in good agreement with the 0.67 value measured by the E00-108 experiment for deuterium and for x=0.32. The z-independence was also confirmed. For x=0.45 PYTHIA gives a value of $R_Y \sim 0.75$. The details of statistical errors assuming the beam time of table 2 are given in table 3 for the yields $Y^{\pi^{\pm}}$, the yields ratio R_Y and the ratio R^D_{meas}. The statistical errors take into account the subtraction of accidental coincidences.

6 Beam time request

Table 4 gives the requested beam time for these measurements. The time on the Al dummy target simulating the cryogenic target windows is taken to be 20% of the time on the deuterium target. We assumed 30-40 minutes per momentum change and 2 hours per polarity change of the HMS spectrometer.

7 Corrections and systematic errors

Because we are measuring the π^- to π^+ production yield ratio on a deuterium target, most sources of uncertainty will cancel out reducing to either a negligible or very small systematic errors. We may classify the sources of error into two categories: the errors independent of the nature of the detected pion like the general experimental conditions (fluctuations in beam current, target boiling, dead time, ...) and the ones dependent on

Activity	Time hours
Data acquisition (LD2 target)	582
Data acquisition (Al dummy target)	120
Polarity changes (7)	14
Momentum changes (6)	4
Total	720 30 days

Table 4: Beam time request for the proposed measurements.

the nature of the detected pion (π^+ or π^-) such as the difference in acceptance due to polarity change, the difference in PID, background subtraction and target window subtraction.

Since we are using a deuterium target and detecting high pion momenta, we expect pion absorption due to πN final state interactions to be the same for π^+ and π^- and cancel out when taking the yields ratio. Pion absorption in the target, target windows and detectors was also found to be small and similar for π^+ and π^-. Radiative corrections are also independent from the detected pion and would not contribute to the error on the yields ratio.

Table 5 summarizes the possible sources of errors and their contributions to the systematic error on the yields ratio R_Y. The systematic error attributed to the luminosity could easily be reduced to 0.3% because we will be using the same beam current for both π^+ and π^- settings. Other sources of systematics include deadtime and endcap subtraction. Because we are interested in π^+ to π^- ratios, we have to make sure that systematic effects that can vary differently for π^+ and π^- are small and under control. No effects were seen related to the polarity change in HMS. An error of 0.1% [21] was attributed to eventual resulting difference in the acceptance. Systematic uncertainty of 0.2% was given to the detection efficiency. Finally, an error of 0.2% was added to eventual difference in tracking efficiency due to the difference in π^+ and π^- rates. We expect the error from target density changes due to target boiling to be negligible especially if the beam spot size on the target is kept larger than 100 micron and the rastering is implemented [22]. We will make regular checks of the beam size to ensure that it does not vary significantly.

The 0.6 % total systematic error on $\Delta(R_Y)/R_Y$ will result into a $\sim$ 2-3 % systematic error on the ratio R^D_{meas} which is comparable to the statistical error.

Error	$\Delta(R_Y)/R_Y$
Luminosity	0.5 %
Dead time	< 0.1 %
Endcap subtraction	0.1 %
Difference in acceptance: π^+ vs. π^-	0.1 %
Detection efficiency	0.2 %
Tracking efficiency	0.2 %
Total error for a single (x,z) bin	0.6 %

Table 5: Sources and estimate of systematic errors on the yield ratio R_Y

8 Expected results

Figure 7 shows the expected uncertainties for our measurements of the CSV term. Both statistical and systematical errors are included. The yellow band shows the systematic error related to our present knowledge of parton distribution functions; especially the non strange sea contribution. The expected precision is quite good for the first exploration of the CSV term and will provide the most precise measurements of valence CSV contributions. Higher x measurements are very time consuming as we have shown in section 5. The systematic errors related to the PDFs can be reduced with additional measurements such as the approved Drell-Yan experiment E906 [23].

Using the method described in the formalism section, we will extract simultaneously the x-dependent term related to CSV and the z-dependent term connected to the fragmentation functions. Figure 8 shows the expected uncertainties on this term for different z values. The solid curve is a prediction by Feynman and Field. They suggested that $\Delta(z) = (1-z)/(1+z)$. Therefore D(z) would behave like z.

From CSV term, on can extract $(\delta d - \delta u)$ contribution. Figure 9 shows the expected uncertainties; both statistical and systematical. The yellow band is the systematical error related to PDFs. The two curves are the prediction by MRST phenomenological fit.

9 Summary

We request 30 days in Hall C to measure semi-inclusive pion production on deuterium in the deep inelastic regime for $Q^2 > 1.0$ GeV^2. The measurements will be done for four z bins; 0.5, 0.55, 0.6, 0.65 and for two x bins; 0.35 and 0.45. For the first time charge symmetry violation valence quark distribution will be directly extracted. These measurements were strongly recommended by theorists due to their very important implications on various subjects that use the phenomenological PDFs. In case the CSV is large, one should probably re-evaluate all phenomenological PDFs, introduce some explicit charge

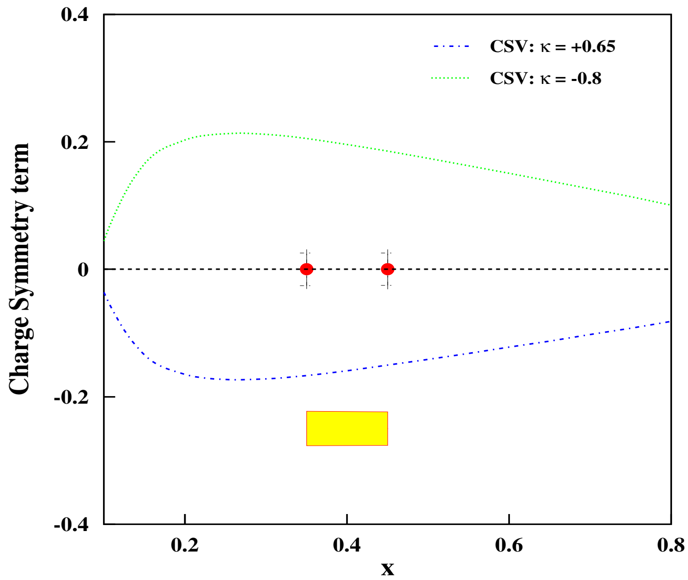

Figure 7: The two curves are the upper and lower limit of CSV contribution given by MRST parameterization. The two points correspond to the expected uncertainties. Both statistical and systematical errors are included. The yellow band corresponds to the systematic error related to our present knowledge of PDFs.

symmetry violation, and re-fit existing cross-sections. One should also review the application of DIS to extract parameters of the Standard Model, since the implicit assumption of charge symmetry in PDFs will introduce problems as suspected for the case of the NuTeV measurements.

References

[1] G.A. Miller, B.M.K. Nefkens and I. Slaus, Phys. Rep. 194 (1990) 1

[2] E.M. Henley and G.A. Miller in Mesons in Nuclei, eds. M. Rho and D.H. Wilkinson (North-Holland, Amesterdam 1979)

[3] G.A. Miller, Nucl. Phys. A 518 (1990) 345; I. Slaus, B.M.K. Nefkens and G.A. Miller, Nucl. Inst. and Meth. B 56/57 (1991) 489

[4] J.T. Londergan and A.W. Thomas, Prog. Part. Nucl. Phys. 41 (1998) 49

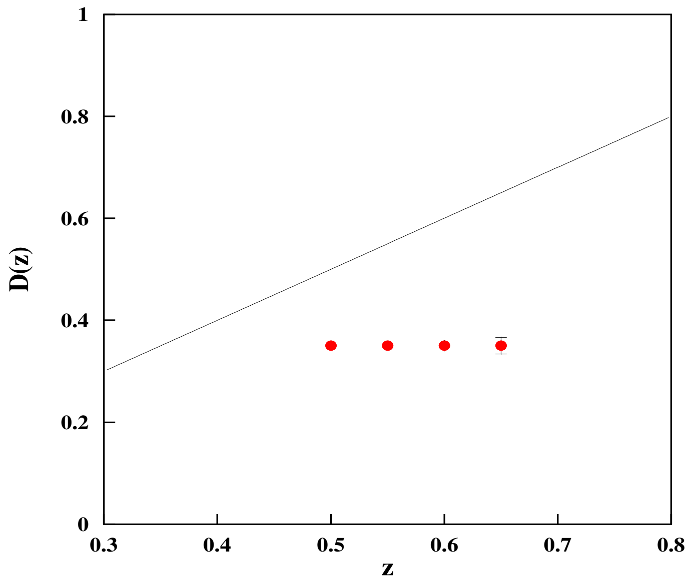

Figure 8: The solid curve is the prediction of D(z) term by Feynman and Field. The points reflect the expected uncertainties. Both statistical and systematical errors are included.

[5] P. Amaudruz et al. (NMC Collaboration), Phys. Rev. Lett. 66 (1991) 2712, Phys. Lett. B 295 (1992) 159

[6] A. Baldit et al. (NA51 Collaboration), Phys. Lett. B332 (1994) 244

[7] E.A. Hawker et al, Phys. Rev. Lett. 80 (1998) 3715, R.S. Towell et al., Phys. Rev. D 64 (2001) 052002

[8] G.P. Zeller et al. (NuTeV Collaboration), Phys. Rev. Lett. 88 (2002) 091802

[9] J.T. Londergan and A.W. Thomas, hep-ph/0407247

[10] K. Ackerstaff et al., Phys. Rev. Lett 81 (198) 5519

[11] K. Hafidi (private communication)

[12] J. Binnewies, B. A. Kniehl, and G. Kramer, Phys. Rev. D 52 (1995) 4947

[13] W.G. Seligman et al. (CCFR Collaboration), Phys. Rev. Lett. 79 (1997) 1213

[14] E. Sather, Phys. Lett. B 274 (1992) 433

[15] E.N. Rodionov, A.W. Thomas and J.T. Londergan, Mod. Phys. Lett A 9 (1994) 1799

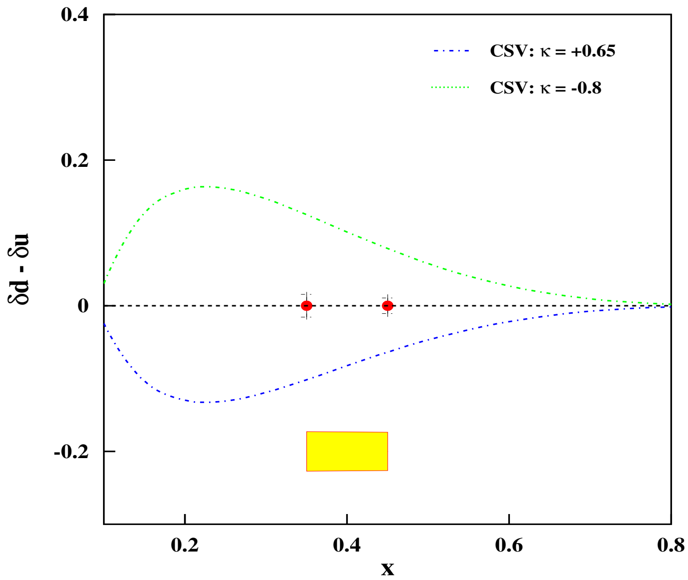

Figure 9: The two curves are the upper and lower limit of $(\delta d - \delta u)$ contribution given by MRST parameterization. The two points correspond to the expected uncertainties. Both statistical and systematical errors are included. The yellow band corresponds to the systematic error related to our present knowledge of PDFs.

[16] A.D. Martin, R.G. Roberts, W.J. Stirling and R.S. Thome, hep-ph/0308087

[17] J.T. Londergan, A. Pang and A.W. Thomas, Phys. Rev. D 54 (1996) 3154

[18] E00-108 experiment, Duality in Meson Electroproduction, Spokespersons: R. Ent, H. Mkrtchyan and G. Niculescu

[19] S. Kretzer, Phys. Rev. D 62 (2000) 054001

[20] H. Mkrtchyan (private communication)

[21] R. Ent (private communication)

[22] E03-103 experiment, A Precise Measurement of the Nuclear Dependence of Structure Functions in Light Nuclei, Spokespersons: J. Arrington and D. Gaskell

[23] E906 experiment, Drell-Yan Measurements of Nucleon and Nuclear Structure with FNAL Main Injector, Spokespersons: D. F. Geesaman and P. E. Reimer